Supporting Information

Kawajiri et al. 10.1073/pnas.0902132106

SI Materials and Methods

Animals. Aryl hydrocarbon receptor (AhR)-deficient ($AhR^{-/-}$) mice (1) were bred under specific pathogen-free conditions and maintained in the animal house of Clea Japan, Tokyo. They were then housed in communal quarters under conventional conditions in the Saitama Cancer Center. Sterilized rodent chow and autoclaved water were provided ad libitum. Germ-free (GF) mice were generated and housed in gnotobiotic isolators under a strict 12-h light cycle in the animal facility in Clea Japan. The C57BL/6J $Apc^{Min/+}$ mice (2) purchased from The Jackson Laboratory were mated with *AhR*-disrupted mice to generate compound $Apc^{Min/+}$·*AhR*-disrupted mice. Progeny were genotyped by an allele-specific PCR assay for the known *Min* nonsense mutation in the *Apc* gene as described previously (3). The loss of Apc^{+} allele in cecal tumors of Min mice was examined using the previously reported method (4), and the loss of heterozygosity (LOH) was found in all tumor tissues irrespective of AhR genotypes.

Tumor Analysis in $AhR^{-/-}$ Mice. In the time course experiment, 114 $AhR^{-/-}$, 29 heterozygous $AhR^{+/-}$, and 35 wild-type $AhR^{+/+}$ mice were killed at the indicated times. The entire intestinal tract of each mouse was then removed and opened along its longitudinal axis. Tumor growth was estimated based on NIH images. After fixation in neutralized 10% formalin for 24 h at room temperature, the intestinal tract was embedded in paraffin, sectioned into slices with 5-μm thickness, stained with hematoxin/eosin (H&E), and examined under a microscope. For the survival studies by genotypes, 138 $AhR^{-/-}$, 92 $AhR^{+/-}$, and 61 $AhR^{+/+}$ mice were used. Tumor analysis in the compound $Apc^{Min/+}$·*AhR*-disrupted mutant mice was performed essentially as described above.

Chemoprevention by AhR Natural Ligands. $Apc^{Min/+}$, compound $Apc^{Min/+}$·$AhR^{+/-}$ mutant, and $AhR^{-/-}$ mice fed with control standard diet F2 (Funabashi Farm), F2-containing I3C (5) (0.1%; Sigma-Aldrich), or F2-containing DIM (0.01%; Wako Pure Chemical) (6) just after weaning of 3–4 weeks of age. Four to 5 mice were used for each time point of the experiment.

Immunohistochemistry and RT-PCR. The anti-AhR antibody developed by R. Pollenz (Clone:17-10) was used for immunohistochemistry. The anti-β-catenin antibody was a mouse monoclonal generated against the C-terminal domain (Clone 14; BD Biosciences). The other antibodies used were as follows: anti-c-myc (Santa Cruz Biotechnology), anti-Ki67 and anti-p53 (DakoCytomation), anti-cytokeratin (CAM5.2, 349205; BD Biosciences), anti-cyp1a1 (Chemicon International), and anti-actin (Sigma-Aldrich). Primers and experimental conditions used to determine the expression of β-catenin, c-myc, cyclin D1, AhR, cyp1a1, and GAPDH were previously reported (7).

Cell Culture, Transfection, and Luciferase Assays. Colon cancer cell lines (DLD-1, SW480, and HCT116), were cultured in DMEM supplemented with 10% FBS at 37 °C in a 5% CO_2 atmosphere. Before the assays were performed, the cells were cultured in phenol red-free DMEM containing 1% charcoal-stripped FBS. For the luciferase assay, cells were transfected with the indicated siRNAs using Lipofectamine 2000 (Invitrogen) according to the manufacturer's protocol. Twenty-four hours after the siRNA transfection, the cells were transfected with 250 ng of the reporter (β-catenin responsive TOPFLASH or nonresponsive FOPFLASH) and 2 ng of pRL-CMV plasmid (control for transfection efficiency), together with 50 ng of the control plasmid or cDNA (β-catenin S37A) (8), and treated with vehicle or ligands (1 μM 3MC or 1 μM βNF) for 24 h, as indicated. Luciferase activity was determined with the Luciferase Assay System (Promega). To nullify nonspecific effects on basal promoters, TOPFLASH reporter activities were normalized against their FOPFLASH reporter activities from parallel experiments.

RNAi. The siRNAs for human AhR (5′- GAACAGAGCAUUUACGAAAUU-3′), CUL4B (5′- CGGAAAGAGUGCAUCUGUAUU-3′), and siCONTROL nontargeting siRNA no. 2 (catalog: D-001210-02-20) were synthesized by Dharmacon. The siRNAs for human adenomatous polyposis coli (APC) (5′- GGAAGUAUUGAAGAUGAAGUU-3′), which target a sequence within exon 2 of APC, was synthesized by Ambion. Cells were transfected with the indicated siRNAs 48 h before the assays.

Antibodies, Immunoprecipitation, and Detection of Ubiquitylated Proteins. Whole-cell extracts incubated with ligands and/or MG132 (10 μM) for 2 h were immunoprecipitated with one of the following antibodies: anti-β-catenin (E-5) or anti-AhR (N-19) (from Santa Cruz Biotechnology), or anti-DDB1 (2B12D1; Zymed Laboratories). For Western blotting, anti-AhR (H-211), anti-ERα (HC20), anti-β-catenin (I-19), and anti-APC (N-15) (Santa Cruz Biotechnology), and anti-CUL4B (9) antibodies were used. To detect ubiquitylated proteins, cells were incubated with ligands and/or MG132 for 6 h, lysed with RIPA buffer (20 mM Tris·HCl, pH 7.5/4 mM EDTA/150 mM NaCl/1% Nonidet P-40/1% deoxycholate/0.025% SDS), and then sonicated. The cell extracts were prepared therefrom, and were immunoprecipitated with the indicated antibodies.

In Vitro Ubiquitylation Assay. The in vitro ubiquitylation assay was performed as described previously (9), with some modifications. The AhR-associated ubiquitin ligase complex was isolated from MCF-7 cells transfected with FLAG-HA-AhR and $CUL4B^{AhR}$ components (HA-DDB1 and myc-TBL3) in the presence or absence of ligands by an anti-FLAG antibody. The immunocomplex was mixed with recombinant GST-β-catenin or recombinant ERα (Calbiochem), E1, E2 mixture, His-ubiquitin, and ATP, and incubated at 30 °C for 1 h. The GST-β-catenin beads were washed twice, and the ubiquitylated proteins were detected by Western blotting. The E3 activity of the purified AhR complex was verified using ERα as a substrate (Fig. S6*C*).

HPLC Analysis of Tryptophan (Trp) Metabolites in Cecal Contents. Cecal contents were collected from 5 GF or control mice and suspended in 50 mM potassium phosphate (pH 7.4) at a ratio of 1 g of feces per 40 mL buffer. After adding an equal volume of ethyl acetate, the mixture was vigorously shaken. After centrifugation, the organic phase and aqueous phase were separately recovered. The organic phase was dried under reduced pressure, and the resulting residue was dissolved in acetonitrile and then applied to an HPLC column under the following conditions: column, YMC-Pack ODS-AM (5 μm) (4.6 × 300 mm) (YMC); UV detection, 280 nm; flow-rate, 1.0 mL min^{-1}; column temperature, 40 °C; mobile phase, a linear gradient of 0–100% acetonitrile aqueous solution with 0.01% trifluoroacetic acid. The aqueous phase was concentrated under reduced pressure and applied to an HPLC column under the same conditions

except for the mobile phase, which consisted of 20 mM potassium phosphate (pH 6.0) (solution A) and a 60% methanol aqueous solution (solution B). Samples were eluted with solution A for 5 min followed by a linear gradient of 0–50% solution B for 20 min.

1. Mimura J, et al. (1997) Loss of teratogenic response to 2,3,7,8-tetrachlorodibenzo-*p*-dioxin (TCDD) in mice lacking the Ah (dioxin) receptor. *Genes Cells* 2:645–654.
2. Moser AR, Pitot HC, Dove WF (1990) A dominant mutation that predisposes to multiple intestinal neoplasia in the mouse. *Science* 247:322–324.
3. Jacoby RF, et al. (1996) Chemoprevention of spontaneous intestinal adenomas in the Apc Min mouse model by the nonsteroidal anti-inflammatory drug piroxicam. *Cancer Res* 56:710–714.
4. Luongo C, Moser AR, Gledhill S, Dove WF (1994) Loss of Apc^{+} in intestinal adenomas from Min mice. *Cancer Res* 54:5947–5952.
5. Xu M, et al. (1996) Protection by green tea, black tea, and indole-3-carbinol against 2-amino-3-methylimidazo[4,5-*f*]quinoline-induced DNA adducts and colonic aberrant crypts in the F344 rat. *Carcinogenesis* 17:1429–1434.
6. Chen I, McDougal A, Wang F, Safe S (1998) Aryl hydrocarbon receptor-mediated antiestrogenic and antitumorigenic activity of diindolylmethane. *Carcinogenesis* 19:1631–1639.
7. Hayashi S-I, Okabe-Kado J, Honma Y, Kawajiri K (1995) Expression of Ah receptor (TCDD receptor) during human monocytic differentiation. *Carcinogenesis* 16:1403–1409.
8. Liu C, et al. (1999) β-Trcp couples β-catenin phosphorylation-degradation and regulates *Xenopus* axis formation. *Proc Natl Acad Sci USA* 96:6273–6278.
9. Ohtake F, et al. (2007) Dioxin receptor is a ligand-dependent E3 ubiquitin ligase. *Nature* 446:562–566.
10. Dharmasiri N, Dharmasiri S, Estelle M (2005) The F-box protein TIR1 is an auxin receptor. *Nature* 435:441–445.
11. Kepinski S, Leyser O (2005) The *Arabidopsis* F-box protein TIR1 is an auxin receptor. *Nature* 435:446–451.
12. Goryo K, et al. (2007) Identification of amino acid residues in the Ah receptor involved in ligand binding. *Biochem Biophys Res Commun* 354:396–402.
13. Tan X, et al. (2007) Mechanism of auxin perception by the TIR1 ubiquitin ligase. *Nature* 446:640–645.

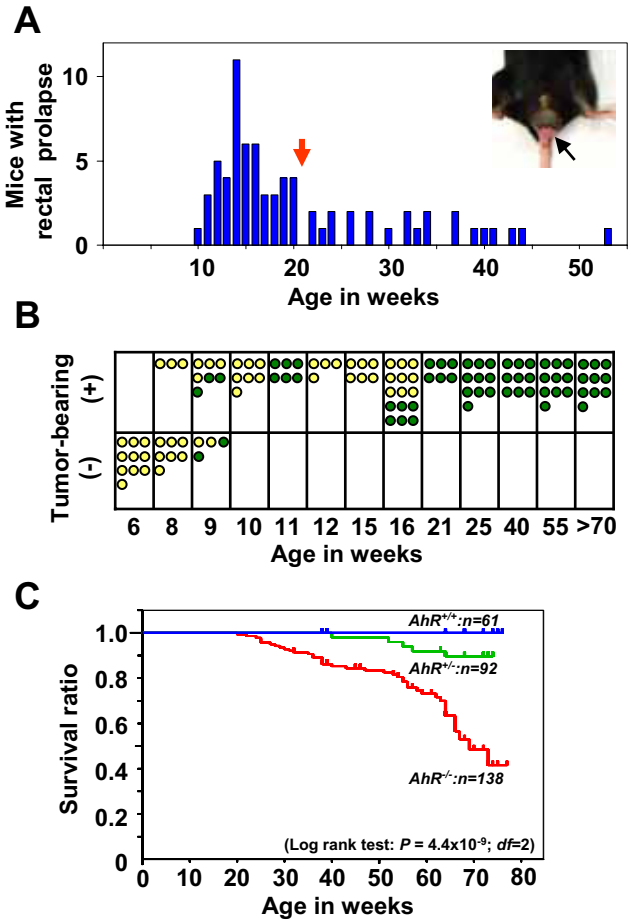

Fig. S1. Cecal tumor development in $AhR^{-/-}$ mice. (*A*) Relationship between the incidence of rectal prolapse (black arrow) and time course by age in weeks in $AhR^{-/-}$ mice. Rectal prolapse was observed in 55% (73/133) of $AhR^{-/-}$ mice with a mean incidence (red arrow) of 20.7 weeks of age. Neither $AhR^{+/-}$ nor $AhR^{+/+}$ mice developed rectal prolapse. (*B*) Macroscopic tumor formation by age in weeks at 2 independent animal houses bred at Saitama Cancer Center (green circles) or Clea Japan (yellow circles). (*C*) Kaplan-Meyer survival curves of $AhR^{-/-}$ mice compared with heterozygous or wild-type littermates. There was no significant difference in survival between $AhR^{+/+}$ and $AhR^{+/-}$ mice ($P = 0.115$).

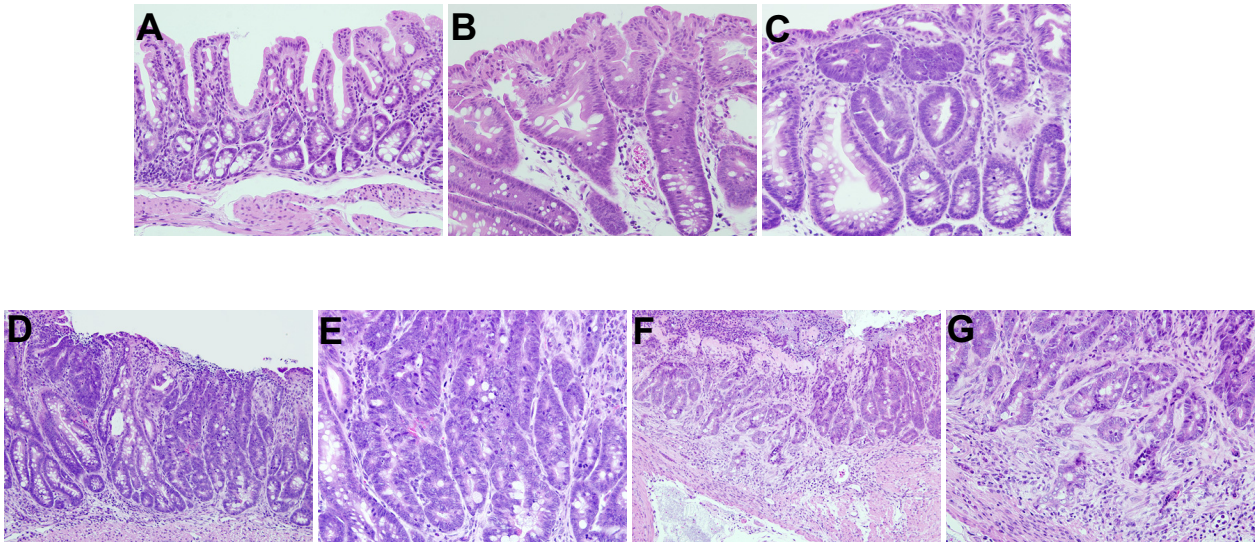

Fig. S2. Representative profiles of histological diagnosis for atypia in $AhR^{-/-}$ mice. (*A*) Normal epithelium (Grade 1), (*B*) mild hyperplasia (Grade 2), (*C*) moderate hyperplasia (Grade 3), (*D*) high grade of atypia, adenoma (Grade 4), and (*F*) adenocarcinoma (Grade 5). Higher magnification sections in *D* and *F* are shown in *E* and *G*, respectively. Tumor invades the submucosal region or beyond as shown in *G*.

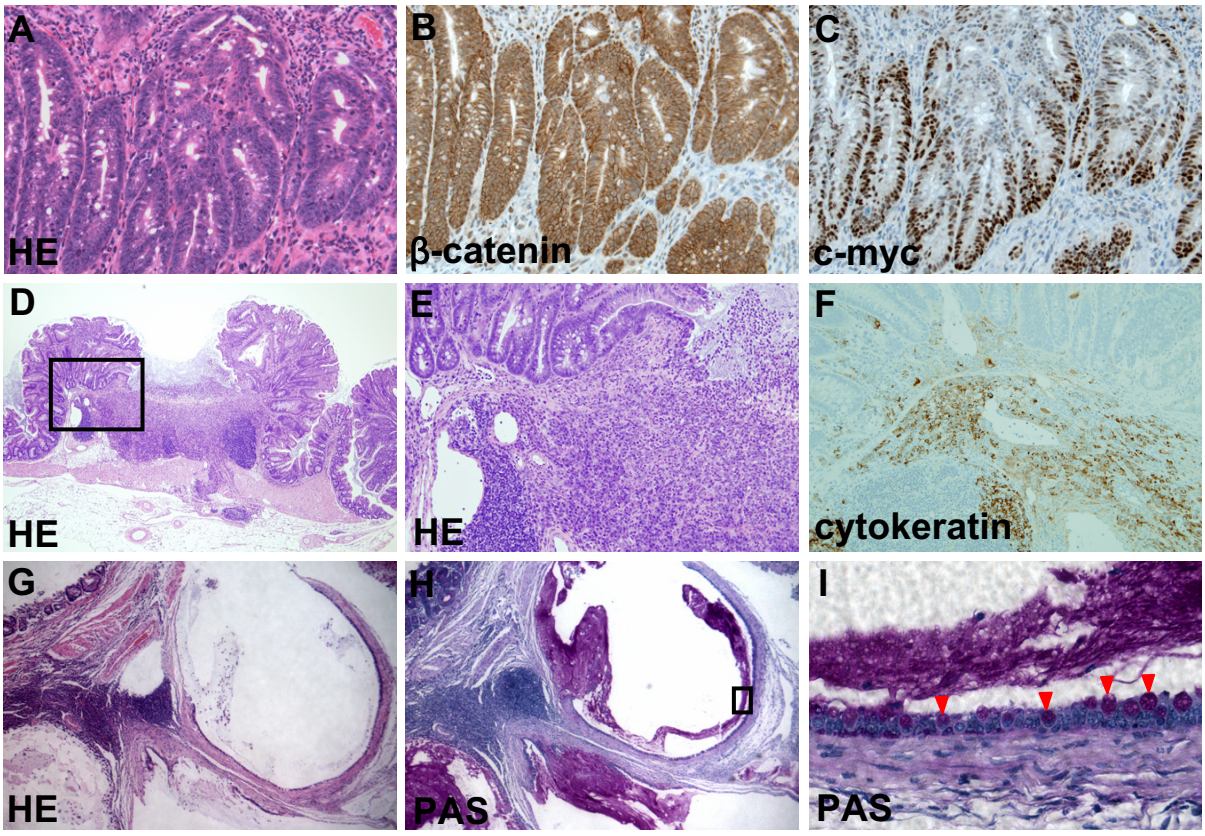

Fig. S3. Adenocarcinomas in the cecums of $AhR^{-/-}$ mice. Representative profiles of well-differentiated (*A*–*C*) and poorly-differentiated (*D*–*F*) adenocarcinomas that developed in $AhR^{-/-}$ mice; a rare case of mutinous adenocarcinoma is also shown (*G*–*I*). H&E staining (*A*, *D*, *E*, and *G*) and immunohistochemical staining with antibodies against β-catenin (*B*), c-myc (*C*), and cytokeratin (*F*), a marker of epithelial cells, are shown. Periodic acid/Schiff-stained sections are also shown (*H* and *I*). Higher magnification sections of the enclosed regions in *D* and *H* are shown in *E* and *I*, respectively. The mucin secretory cells are clearly shown (*I*) (red arrowheads).

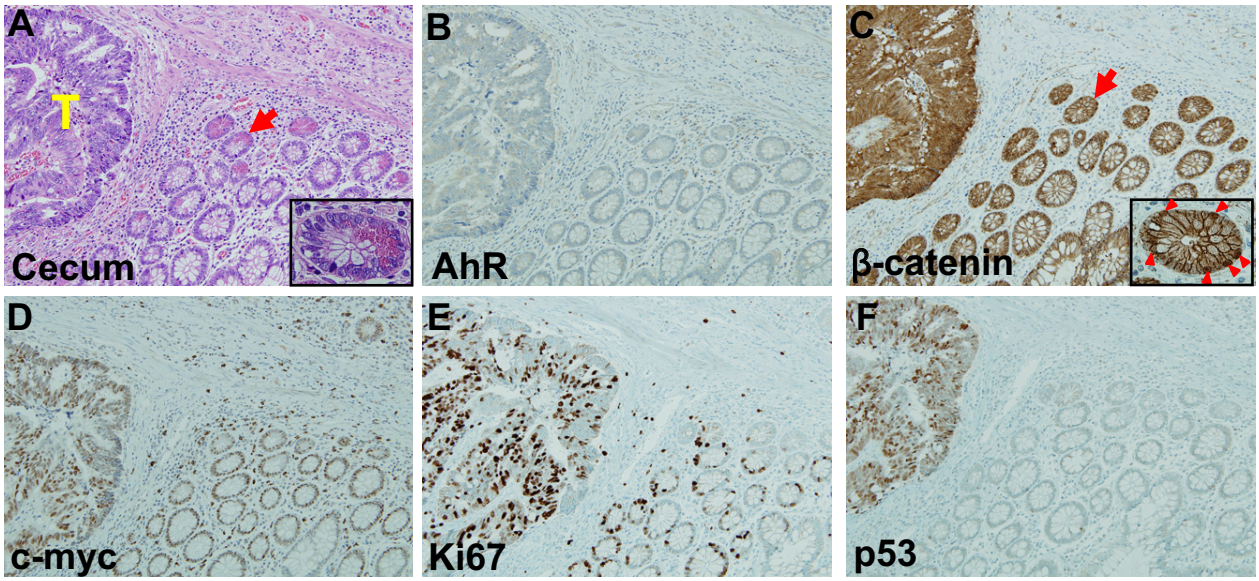

G

Cecal Cancers				AhR expression in normal	
AhR Downregulation	β-Catenin* Overexpression		p53** Overexpression	Ileum	Colon
12/12	12/12	C>N : 4 C=N : 4 C<N : 4	7/12	12/12	12/12

Fig. S4. Expression of AhR and β-catenin in human cecal cancer. H&E (*A*) and immunohistochemical staining of cecal cancer (shown by T) and surrounding tissues with antibodies against AhR (*B*), β-catenin (*C*), c-myc (*D*), Ki67 (*E*), and p53 (*F*) are shown. A magnified inset of a crypt indicated by the red arrow is also included in the panel of H&E and β-catenin staining. (*G*) Down-regulation of AhR expression and abnormal accumulation of β-catenin in cecal cancer specimens from 12 patients. *, the subcellular localization of β-catenin was classified into 3 categories according to the immunohistochemical staining: C > N for predominantly cytoplasmic (membranous) distribution; C = N for equal cytoplasmic and nuclear distribution; and C < N for predominantly nuclear localization. **, immunohistochemical detection of p53 protein was considered positive when at least 20% of the cells had stained nuclei.

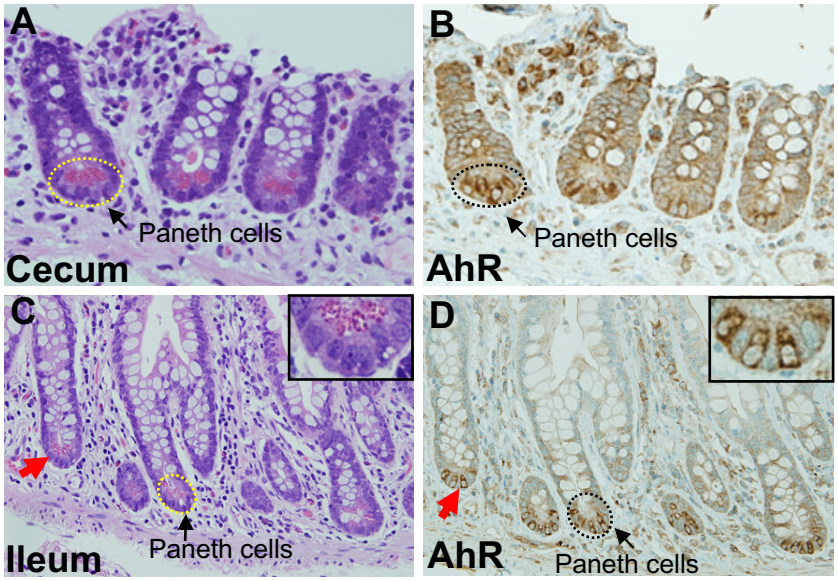

Fig. S5. Expression of AhR in Paneth cells of the human intestine. (*A* and *C*) H&E staining of human intestines. Paneth cells enclosed by the dotted line were observed in the normal cecum (*A*), as well as in the ileum (*C*). AhR expression in the cecum (*B*) or ileum (*D*) is shown. A magnified inset of a crypt, indicated by the red arrow, is also included in *C* and *D*.

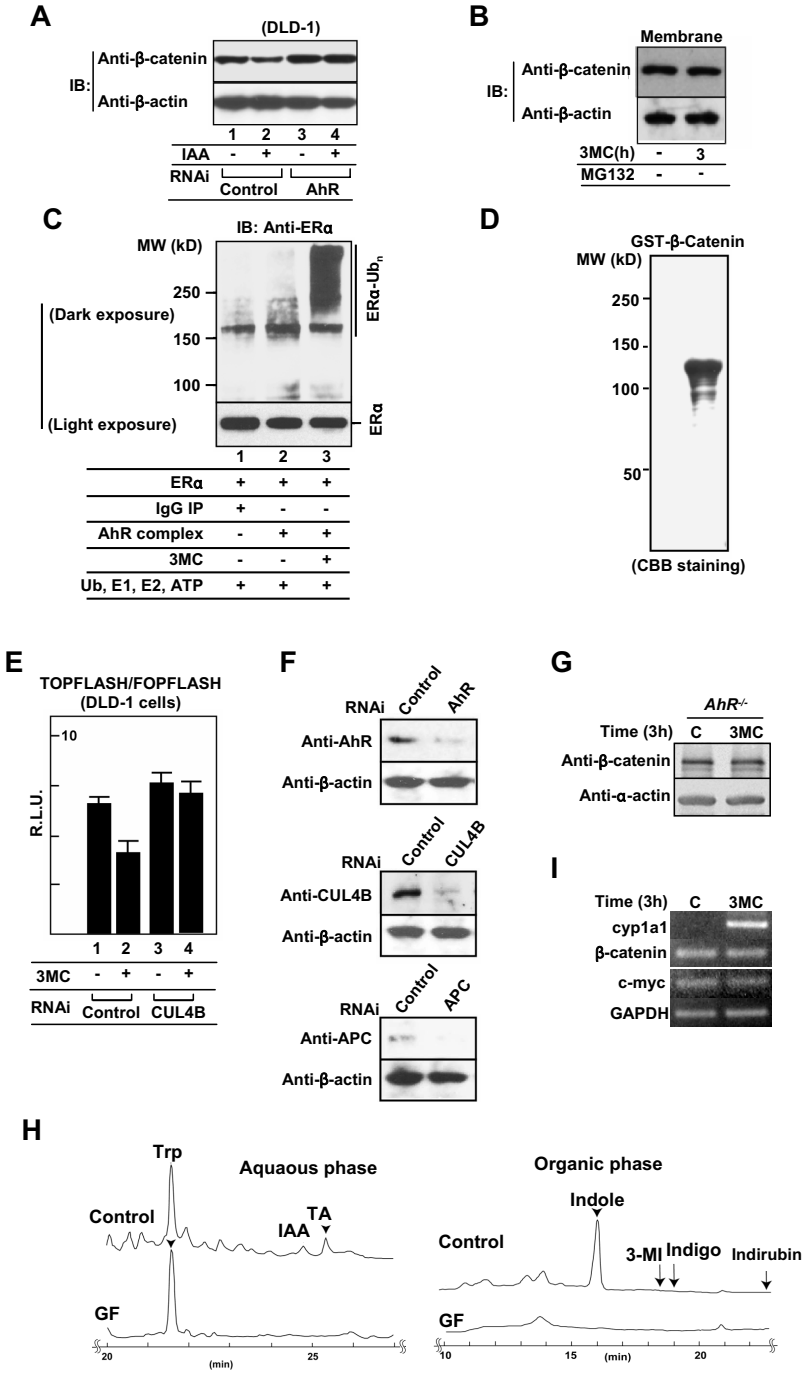

Fig. S6. AhR ligand-dependent degradation of β-catenin. (*A*) Effect of IAA on β-catenin degradation is AhR-dependent. DLD-1 cells transfected with the indicated siRNAs were incubated with IAA for 6 h, lysed, and then analyzed by Western blotting. (*B*) Level of membranous β-catenin is unchanged by an AhR ligand. The membranous fraction from DLD-1 cells incubated with or without 3MC for 3 h was analyzed by Western blotting. (*C*) To verify E3 activity in the purified AhR complex, the FLAG-HA-AhR-associated immunocomplex was mixed with recombinant ERα and His-ubiquitin, and an in vitro ubiquitylation assay was performed. Polyubiquitylation of ERα was determined by Western blotting using an anti-ERα antibody. (*D*) Recombinant GST-β-catenin was purified using glutathione beads and analyzed by CBB staining. (*E*) AhR represses the transactivation function of endogenous β-catenin. DLD-1 cells were transfected with the reporter plasmid and incubated with ligands as indicated to determine the transactivational activity of endogenous β-catenin. All values are means ± SD for at least 3 independent experiments. (*F*) The knock-down efficiency of AhR, CUL4B, and APC in DLD-1 cells in Fig. 3*F* was determined by Western blotting. (*G*) *AhR*$^{-/-}$ mice received a single injection of 3MC (4 mg/kg), and were killed 3 h after the injection. The levels of β-catenin in the cecum were detected by Western blotting. (*H*) HPLC analysis of the cecal contents of control specific pathogen-free or GF mice. Arrows and arrowheads indicate the retention times of authentic standards of Trp and its metabolites, respectively; 3-MI, 3-methyl-indole. (*I*) Messenger RNA expression in the cecal epithelium in control or 3MC-treated mice 3 h after injection.

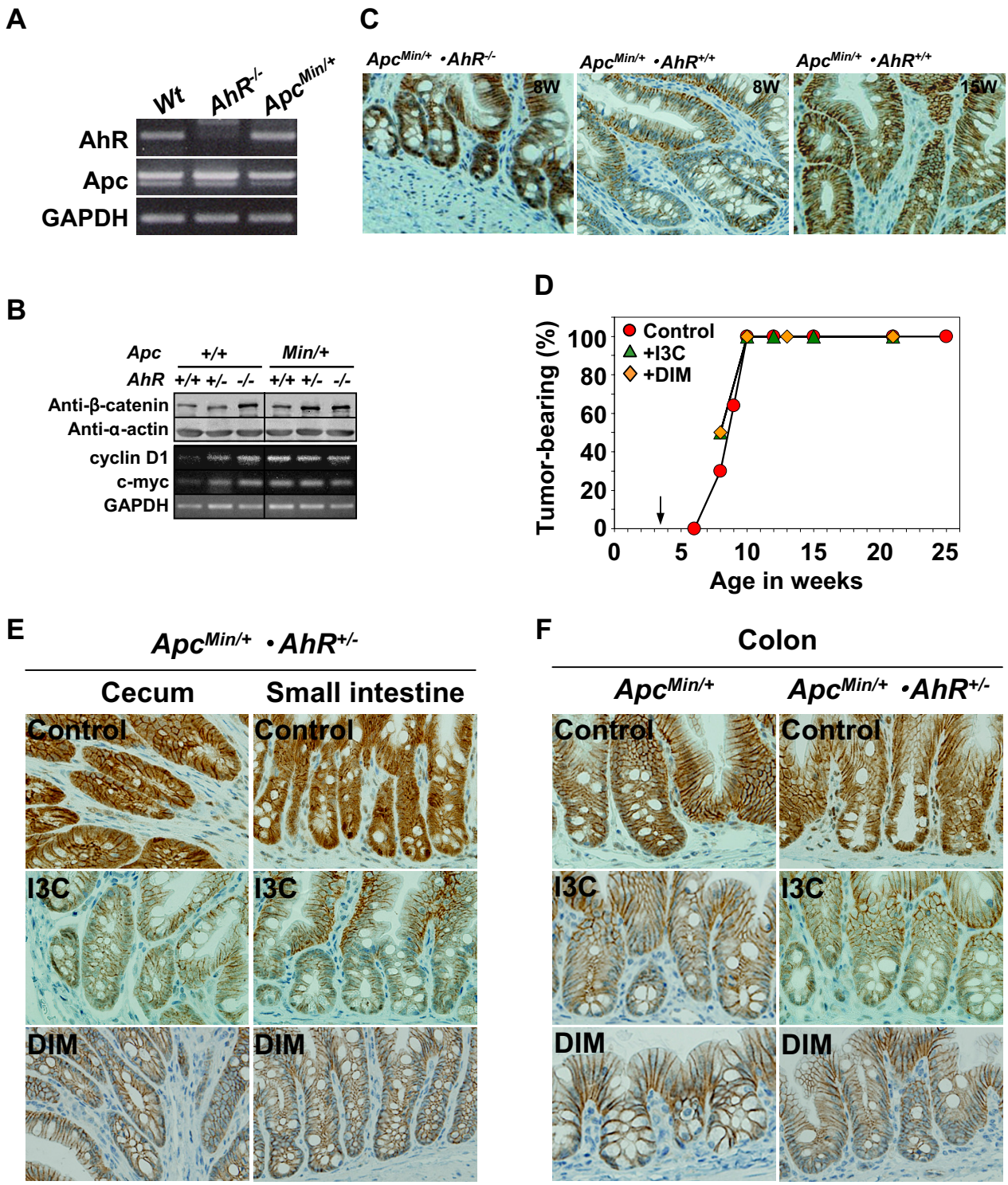

Fig. S7. Effect of AhR natural ligands on the accumulation of β-catenin in the intestines. (*A*) Expression of AhR and Apc mRNAs in the normal cecum of $AhR^{-/-}$ or $Apc^{Min/+}$ mice. (*B*) Levels of β-catenin protein and its downstream gene expression profiles in the cecal epithelium. The cecal epithelium from 6-week-old compound mutant mice was used. Western blotting and RT-PCR results are representative of 3 independent experiments. (*C*) Representative profile of immunohistochemical staining with an antibody against β-catenin in the cecal epithelium from $Apc^{Min/+}{\cdot}AhR^{+/+}$ and $Apc^{Min/+}{\cdot}AhR^{-/-}$ mice. (*D*) Cecal carcinogenesis in the $AhR^{-/-}$ mice. Tumor development in mice fed a control diet (red circles), 0.1% I3C-containing (green triangles), or 0.01% DIM-containing (beige diamondes) diet just after weaning of 3–4 weeks of age as noted by the arrows. (*E*) Representative profile of immunohistochemical staining with an antibody against β-catenin in the cecum or small intestine from 12-week-old $Apc^{Min/+}{\cdot}AhR^{+/-}$ mice fed a control or AhR ligand-containing diet. (*F*) Representative profile of immunohistochemical staining with an antibody against β-catenin in the colon of from $Apc^{Min/+}$ or $Apc^{Min/+}{\cdot}AhR^{+/-}$ mice fed a control or AhR ligand-containing diet.

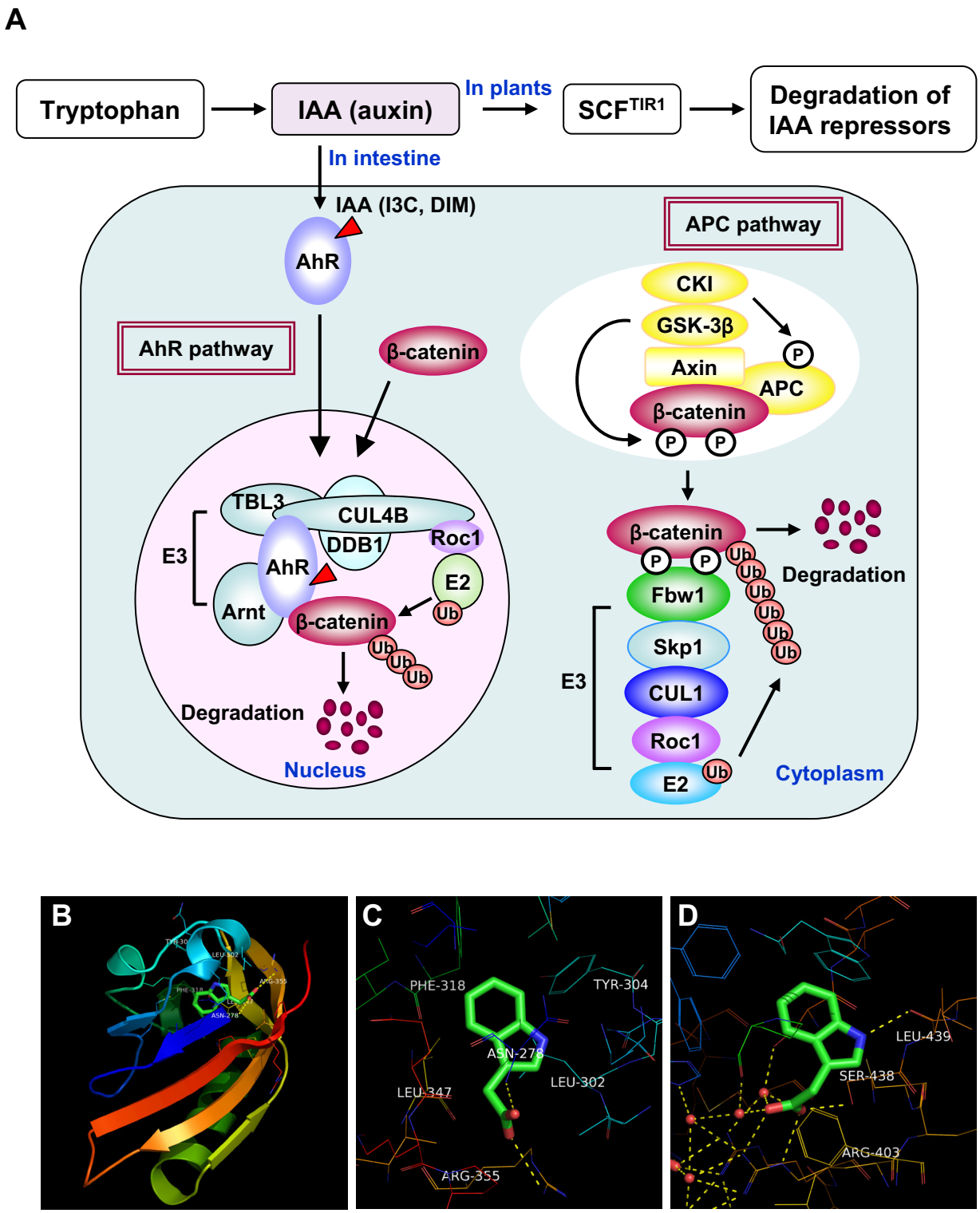

Fig. S8. AhR-directed β-catenin degradation. (*A*) Schematic representation of β-catenin degradation by a novel AhR ligand-dependent E3 ubiquitin ligase complex. IAA (auxin) induces degradation of Aux/IAA transcriptional repressors via the auxin receptor SCF^{TIR1} in plants (10, 11), whereas it has a role as a physiological ligand in the degradation of β-catenin via the $CUL4B^{AhR}$ complex in the intestine. (*B*) Ribbon-style drawing of the AhR PAS-B domain and binding of IAA. Model of IAA in the binding site of the AhR PAS-B domain (*C*) or TIR1 (*D*). Computer simulation using Glide 4.0 and Prime (Schrödinger) suggests that AhR (12) and TIR1 (13) accommodate IAA in their ligand-binding domains in similar manners between interactions of Arg-355 of AhR (*B* and *C*) and Arg-403 of TIR1 (*D*) with IAA, supporting a role of IAA as a natural ligand for AhR.